Exploring the Role of Carbon Nanosheets for Detoxification of Cr(VI) from Aqueous Solution

Kant Madhur[1], Khatoon Fehmeeda[2] and Sen Mousumi[1*]
1. Department of Chemistry, Amity Institute of Applied Sciences, Amity University Uttar Pradesh, Noida – 201313, INDIA
2. Department of Chemistry, Jamia Milia Islamia, University, Delhi, INDIA
*msen@amity.edu

Abstract

Toxic pollutants in wastewater must be reduced in order to protect the aquatic ecosystem's stability and the public's health. Finding affordable and effective technologies for treating municipal, horticultural, aquacultural and industrial wastewater is urgently needed. Nitrogen-doped carbon nanosheets (N-CNS), which are produced by hydrothermal reaction from glycerol, sulfuric acid and melamine, have strong adsorptive behaviour against hazardous aqueous pollutants such as heavy metals and organic compounds. The overall elemental composition of CNS is altered by nitrogen incorporation, favouring CNS interaction with pollutants. The objective of the current investigation was to investigate the possibility for Chromium(VI) [Cr(VI)] adsorption on the CNS from a liquid solution.

The ideal pH for Cr (VI) adsorption was noted to be 2.0. The Cr(VI) adsorption was enhanced when the starting metal concentration is more up to 700 mg L^{-1}*. A maximum removal of 256.41 mg* g^{-1}*was seen when pH was 2.0 at 700 mg* L^{-1} *initial Cr(VI) concentration. We employed both the Freundlich and the Langmuir adsorption isotherms to determine the adsorption equilibrium constants. Using fitting curves and correlation coefficients (*R^2*), it has been found that the model of the Langmuir isotherm is a best fit and it indicates homogeneous surface of CNS.*

Keywords: Chromium (VI), Carbon nanosheets, Specific metal uptake, Detoxification.

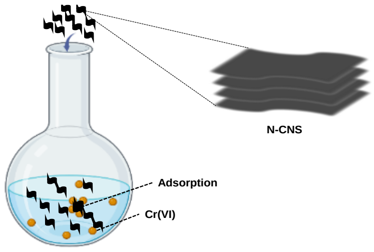

Graphical Abstract

Introduction

For humans and other animals, water is a definite necessity. However, when hazardous chemical components build up in aquatic environments on account of human activity, the aquatic value of waterways and ponds is decreasing. Hazardous chemicals such as organic fertiliser and heavy metals, have an influence on the biological population and aquatic life.[1]

Chromium (VI) is among the dangerous heavy metals coming from aqueous waste streams[2] of many industries in the form of chromate (CrO_4^{2-}) and dichromate ($Cr_2O_7^{2-}$) such as metal cleaning, plating and processing of metals, production of anticorrosive agents, preservation of wood, processing of wood, preparation of alloys, production of pigments, tanning of leather, production of dyes, printing etc.[3-8] Since Cr(VI) stays in the environment permanently and renders remediation extremely challenging, this presents an unacceptable associated pollution .As a result of its tenacious tendency, it enters the food chain, reaching dangerous amounts in living things over time and posing major health risks such as lungs and stomach discomfort, digestive tract cancer, poor plant growth rates and animal mortality etc. Therefore, it is urgent and important to remove it from waste water before being released into sewage systems, adjacent landmasses, or natural water systems.

Chemical reduction and caustic soda precipitation are the traditional physico-chemical processes used to remove Cr(VI). This method utilizes an enormous quantity of chemical substances and produces an abundance of sludge whereby disposal culminates in secondary contamination. Other available treatments include electrolysis, ion exchange and reverse osmosis, amongst many others, that are both expensive and high energy operations but also poor in eliminating metal ions that are present in enormous quantities of wastewaters at trace levels.[9] Consequently, it is essential to develop environmentally responsible methods and technologies that can clean the environment without producing hazardous waste byproducts.

In this quest, adsorption provides a simple, economical and practical technique of treating wastewater with contaminants removal efficiency of 90 to 99%.[10] Adsorption includes the holding capacity and immobilization of adsorbate, the exterior of adsorbent *via* chemical (bond sharing) and physical (Van der Waals) interactions. Hence, it is interesting to develop adsorption-based water treatment skills to alleviate toxic metals, dyes and other organic pollutants. Herein, we have synthesized CNS, an eco-friendly adsorbent for wastewater treatment via hydrothermal reaction of glycerol, H_2SO_4 and melamine.

As an adsorbent, CNS has vital characteristics such as porous morphology, large surface area and surface functional groups.[11] There has already been a thorough assessment of properties of adsorption of CNS with various preparation and modification processes.[12,13] Interest in CNS alteration through nitrogen doping has grown recently. Due to the difference in electronegativity, the addition of heteroatoms like nitrogen to the ordered sp^2- hybridised graphite structure changes the electrical charges inside the original π-electron network. For instance, nitrogen doping (N-doping) has been demonstrated to boost the detection limit of sensors, to facilitate the dispersion of nanomaterials and to improve the catalytic capabilities of nanocarbon.[14]

N-doping on the CNS surface enhances electron mobility. Findings indicated that urea treatment promoted graphitic-N formation while melamine treatment was advantageous for pyridinic-N and pyrrolic-N creation.[15] Pyrrolic-N, pyridinic-N, amine-N, amide-N, nitrile-N and other organic forms of nitrogen are located in the central nervous system.[16,17] The heat stability of organic N-functional groups is very high. The most stable of them are quaternary-N, pyridinic-N-oxide, pyridinic-N and pyrrolic-N.[18,19]

Considering how permeable are the adsorbents, is also crucial because it creates a pathway for pollutants to diffuse from a liquid or gaseous to the solid phase adsorbents. Additionally, N-doping improves the CNS surface's basicity which aids in electrostatic attraction.[20] This makes N-CNS a promising commercial adsorbent by encouraging the taking in of a number of pollutants on it. N-doping creates basic sites that offer unpaired electrons for complicated metal synthesis.

As a result, N-CNS possesses high affinity for adsorption for heavy metals. Moreover, by inserting the lone pair electron of nitrogen in the aromatic system, heterocyclic compounds like pyrrole also positively contribute to cation-bonding. Due to nitrogen's electronegativity, pyridine, which does not contribute to aromaticity, weakens the capacity of cations to attach to the aromatic ring.[21]

In the current research, Cr(VI) adsorption was assessed using the batch data at an alternate initial Cr(VI) concentrations and with varying pH values. Data on equilibrium adsorption were tested with both the Langmuir and Freundlich adsorption isotherms and the nature of biosorption is also discussed.

Material and Methods

Synthesis of N-CNS. The synthesis of CNS was achieved via hydrothermal reaction using melamine (Merck), sulphuric acid (Merck) and glycerol (Fisher Scientific) as discussed earlier.[12] The synthesized CNS was dispersed in distilled water and sonicated at room temperature for 25 minutes to eliminate aggregates before use.

Characterization techniques. CNS was observed using SEM (SU8010, Hitachi, Japan) and HRTEM (JEOL, JEM-2100F) at an acceleration voltage of 200 kV. At IUAC in New Delhi, tapping mode on a nanoscope (IIIa) was used for Atomic force microscopy (AFM) analysis. Using the Belsorp max instrument, the adsorption-desorption isotherm of N_2 was achieved at 77 K. At the Indus 2 synchrotron radiation source in Indore, observations using the X-ray photoelectron spectroscopy (XPS) technique were made.

Preparation of Cr(VI) solutions: The Cr(VI) solutions of different concentrations [50-1000 mg Cr(VI)/L] were prepared by diluting a stock solution [2.82 g Cr(VI)/L] prepared by dissolving the required quantities of solid potassium dichromate ($K_2Cr_2O_7$) in deionized water.

Batch Adsorption studies: The adsorption experiments/ trials were run in a batch mode in order to research adsorption behaviour of Cr(VI) on the synthesized CNS. For the equilibrium and adsorption kinetics studies, a weighed amount of the adsorbent (100 mg on dry wt. basis) was introduced to the flask containing 100 mL of a known concentration of Cr(VI) solution. Before adding the adsorbent, 1 N H_2SO_4 solution was used to bring the pH of the solution containing Cr(VI) to the desired level. The solution was kept in an orbital shaker at 180 rpm for 12 h at 30 ºC. Samples were periodically taken out and centrifuged for 15 minutes at 5000 rpm. The residual Cr(VI) content in the liquid supernatant after separation was measured. The Cr(VI) adsorption efficiency (% removal) and adsorption capacity (qe, mg/g) were determined by equations 1 and 2:

$$q_e = (C_i - C_e) / M * V \tag{1}$$

% removal efficiency of Cr(VI)

$$= \frac{C_i - C_e}{C_i} \times 100 \tag{2}$$

where Ci represents the starting concentration (in mg/L) and Ce represents the equilibrium concentration (in mg/L),The sample's mass is M (g) and the Cr(VI) solution's volume is V(L).

Similar methods were used in each batch experiment to investigate the effects of pH (2–9), initial Cr (VI) concentration (50–1000 mg Cr(VI)/L), adsorbent dose (0.5–4.0 g/L) and contact time (0-700 minutes). All experiments were performed in triplicate and average values are presented.

Assay techniques. The residual Cr(VI) concentration was determined spectrophotometrically (Aquamate, UV-VIS Spectrophotometer) at 540 nm using Di-Phenyl Carbazide (DPC) as the complexing agent (Standards methods for determination of water and wastewater, American Public Health Association (APHA, 1989).

Results and Discussion

SEM photos of CNS (Figure 1a, b) exhibited thin graphitic sheets with folded structure. The HRTEM image of CNS (Figure 1c-e) exhibited the layered and porous morphology of the as-synthesized CNS, suggesting its amorphous nature. Furthermore, AFM images confirm the height profile of the as-synthesized CNS to lie in the 1-4 nm range (Figure 1f).

The persistence of the C 1s, O 1s and N 1s peaks at 286.2, 402.1 and 532.4 eV respectively represent the most XPS survey peaks (Figure 2a). Two prominent peaks at binding energies of 403.8 and 404.8 eV are visible in the deconvoluted spectra of N 1s, confirming pyrrolic and pyridinic N respectively (Figure 2b).

Effect of initial pH: In experiments on adsorption, the initial pH's optimization seems to be significant.The pH of the solution influences both the surface charges of adsorbents and the distinct forms of ionic chromium -based forms. Figure 3 displays influence of initial pH (2-9) about the absorption capacity and % removal of Cr(VI) on the CNS adsorbent.

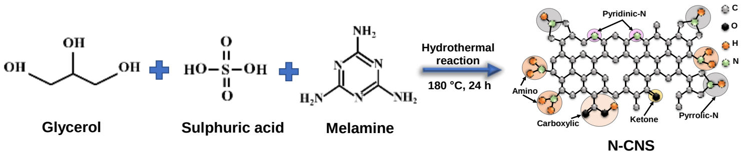

Scheme 1: Synthesis of N-CNS

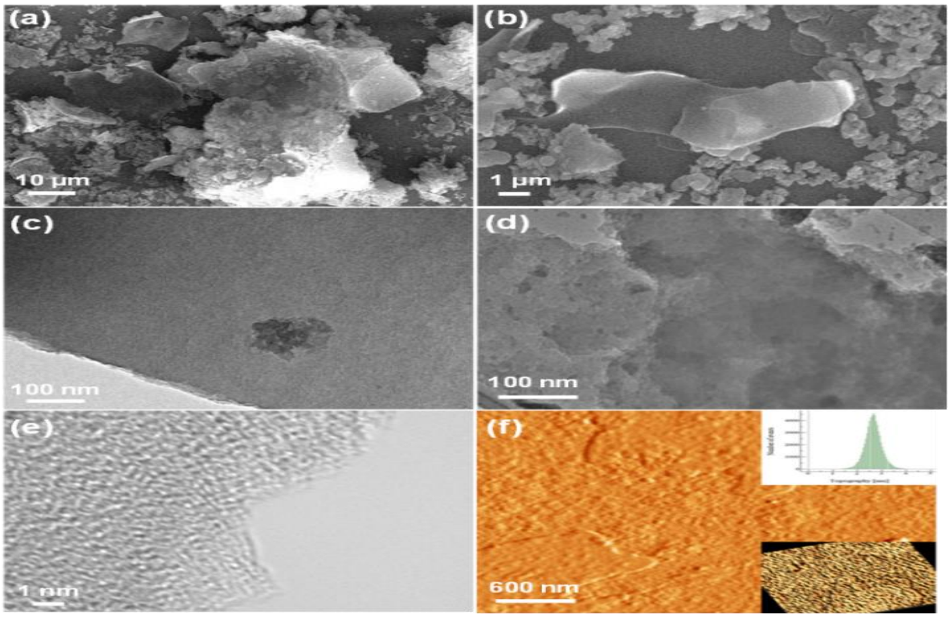

Figure 1: Microscopic images of N-CNS. (a, b) SEM images, (c-e) TEM images and (f) AFM images.

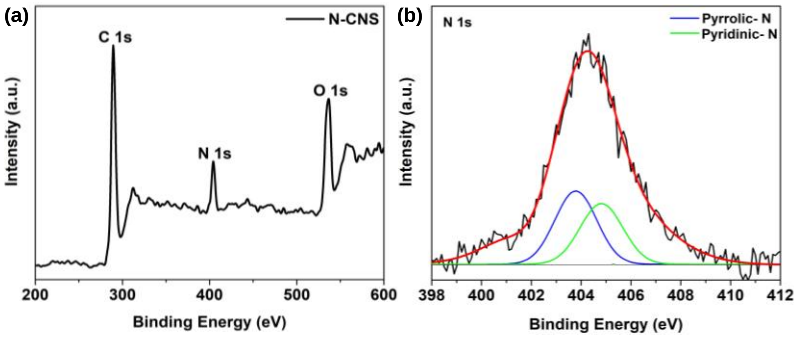

Figure 2: XPS analysis of N-CNS. (a) Survey spectra and (b) Deconvoluted spectrum of N 1s.

The maximum capacity for Cr(VI) adsorption on the CNS nanocomposite occurred at pH 2.0, implying that the mechanism of adsorption of the material for Cr(VI) was strongly pH-dependent. The removing effectiveness fell off quickly as raising the pH. The majority of Cr(VI) appears in anionic form ($HCrO^{4-}$) at an initial pH of 2.0 which could be successfully captured by the exterior of the CNS nanocomposite which is positively charged by electrostatic attraction. Consequently, according to the pH analysis, the electrostatic interaction between the oppositely charged CNS nanocomposite surface and anionic $HCrO^{4-}$ is what facilitates the absorption process. The figure shows a sharp decrease of adsorption capacity of Cr(VI) from 16 mg Cr(VI)/g to 12.8 mg Cr(VI)/g accompanied by a rise in pH range: 2 to 5.

The higher supply of hydrogen ions available for protonation of the operative groupings in cellular wall is the reason for the higher Cr(VI) removal at lower pH, enhancing the interaction between the protonated cell functional groups and the negatively charged dichromate anions. The ideal pH for the increased adsorption of Cr (VI) by CNS adsorbent was estimated to be 2.0.

Effect of contact time on Cr(VI) removal: Figure 4 demonstrates the influence of contact time variation (from 0 to 700 minutes) on adsorption performance. For Cr(VI) concentrations (100 mg/L), dosage of 1 g/L at 30 °C and shaking speed of 180 rpm, the effect of contact time was assessed. 60% of the Cr(VI) was removed after 60 minutes of maximum Cr(VI) adsorption. Since there was not an active site for Cr(VI) ions to be adsorbed, the amount of Cr(VI) adsorbed onto the CNS increased as the contact duration increased up to 60 minutes and the adsorption capacity reached equilibrium. So, during the experimental trials, a contact time of 60 minutes was determined to be ideal. After 420 minutes, a marginal decease in removal was observed till 700 minutes.

Impact of Dose on Cr(VI) removal: Effects of the adsorbent dose on removal potential of Cr(VI) were studied by incorporating various amounts of CNS (0.1-4.0 g/L) in 100 mg/L Cr(VI) solution for 1 h shaking time in shake flask (180 rpm) at pH 2 separately. Results are displayed in figure 5. The removal capacity is improved from 28 to 96 mg by increasing the dose of the adsorbent from 0.1 to 2.5 g. This might be understood that additional active adsorption sites are brought about by an increase in adsorbents. Since, beyond the proportion of 2.5 g/L, complete removal was observed, demonstrates that adsorbent quantities may not be significantly increased after reaching their greatest value if they are raised further. In our tests, 1.0 g of sustained adsorbent dosage was enough to remove Cr (VI).

Effect of initial Cr(VI) concentration: Figure 6 shows the effects of different initial Cr(VI) concentrations (50-1000 mg/L) on the removal capacity by addition of 1.0 g of CNS in a metal ion solution having pH 2. The adsorption capacity is drastically raised from 44 to 240 mg/g by raising the starting concentration from 50 to 700 mg/L. The inability to attain CNS surface saturation at low Cr(VI) concentrations can be attributed to this. The gradual colonisation of active sites will result in greater removal capacities as the concentration of metal ions rises.

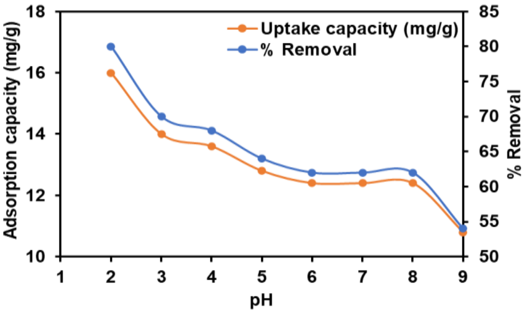

Figure 3: Effect of initial pH on adsorption of N-CNS.

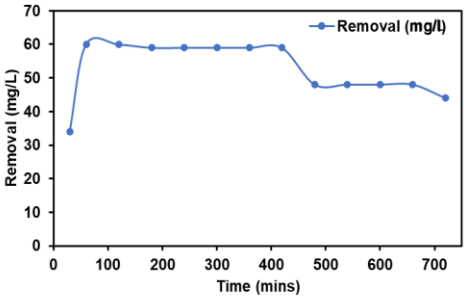

Figure 4: Role of contact time on the percentage of Cr (VI) removal on CNS.

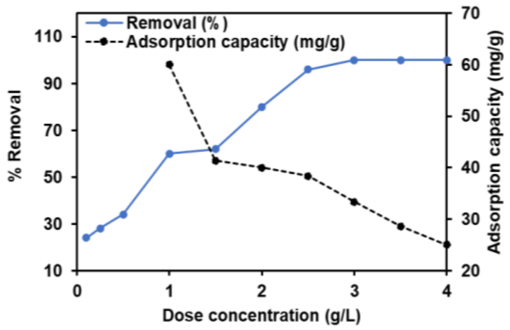

Figure 5: Concentrations of adsorbent on adsorption of Cr(VI)

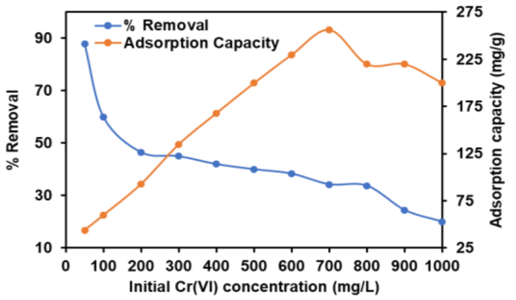

Figure 6: Effect of initial Cr(VI) concentration.

However, due to the limited number of empty sites on the CNS, the rate of increase in adsorption capacity is delayed when the starting concentration is higher than 700 mg/L. However, the % removal was discovered to be maximum of 88% at 50 mg/L concentration which was found to be only 20% at 1000 mg/L initial Cr(VI) concentration.

Adsorption Isotherms: The Langmuir adsorption isotherm model states the relationship at a steady temperature between the amount of metal ions extracted by the adsorbent and the unadsorbable component in solution as follows:

$$q_e = \frac{Q^0\, b\, C_e}{1 + b\, C_e} \tag{3}$$

$$\frac{1}{q_e} = \frac{1 + b\, C_e}{Q^0\, b\, C_e} \tag{3a}$$

$$\frac{C_e}{q_e} = \frac{1 + bC_e}{Q^0 b} = \frac{1}{Q^0 b} + \frac{C_e}{Q^0} \tag{3b}$$

where qe is the number of metal ions absorbed per gram by the adsorbent at equilibrium [mg Cr(VI)/g of adsorbent] and Ce is the metal ion concentration at equilibrium after sorption, still existing in the solution (mg Cr(VI)/L). Theb and Q^o, Langmuir constants, denote the affinity between the binding sites and the maximum quantity of Cr(VI) ion attached per gram of sorbent to create a monolayer.[2] The plot's (Ce/qe against the residual concentration Ce), intercept and slope are can be used to compute the values of Q^o and b.

For the adsorption of Cr(VI) on a heterogeneous surface, the Freundlich adsorption isotherm is written as:

$$q_e = K_F C_e^{1/n} \tag{4}$$

$$\log q_e = \log K_F + \frac{1}{n} C_e \tag{4a}$$

where K_F and n which correspond to the adsorbent's capacity for adsorption and its intensity for adsorption respectively, are the Freundlich constants. The Freundlich constants n and K_F can be calculated from the slope and intercept of eq. 4 in logarithmic form which are equal to 1/n and K_F respectively.

The experimental data defining the adsorption equilibrium of Cr(VI) was used in this study to test both the Langmuir and Freundlich adsorption isotherms and to demonstrate the CNS's capacity for Cr(VI) adsorption. The Cr(VI) adsorption data collected at various initial Cr(VI) concentrations (50-1000 mg/L), pH 2.0 and 30^0C respectively, are used to create the Langmuir and Freundlich adsorption isotherms shown in figures 7 and 8 respectively. The slopes, intercepts and regression coefficients of the straight lines depicted in figures 7 (Langmuir isotherm) and 8 (Freundlich isotherm) were used to derive the values of the adsorption isotherm constants. The highest quantity of adsorbed Cr(VI) per gramme of adsorbent (CNS) to form a full monolayer on the surface was 256.41 mg and the adsorption affinity 'b' for binding of Cr(VI) on the adsorbent sites was 0.09, according to the Langmuir adsorption constant Q0 estimated in the current work (L mg^{-1}).

These findings show that Cr(VI) is strongly bound to the adsorbent surface. The intercept and slope of the Freundlich adsorption isotherm were used to calculate the adsorption capacity (K_F) and adsorption intensity (n), which were 9.55 and 2.56 respectively. Regarding the linear regression coefficient values (R^2), the experimental data and the Freundlich and Langmuir models were in good agreement.

However, a greater R^2 value in the Langmuir model led to a better match of the adsorption data. For monolayer adsorption, both models can be used. The Freundlich model, on the other hand, uses several binding points that are heterogeneously spread across the adsorbent surface to provide a more realistic description of adsorption by the adsorbent. The Langmuir model, in contrast, depicts the adsorption onto a surface that includes a small number of identical sites evenly distributed throughout the adsorbent surface.

The Langmuir isotherm model is the best fit and implies that the surface of the CNS is probably of a homogeneous nature based on correlation coefficients (R^2) and fitting curves. The maximum adsorption capacity was 256.41 mg g^{-1}, surpassing some of the previously reported adsorbents (Table 1).

Table 1
Adsorption capacity of CNS for Cr(VI) in comparison to other reported different adsorbents[2]

Adsorbent	q_e (mg/g)
Synthetic polymers[22]	156
Carbon nanotubes (CNTs)[23]	9.50
Composite chitosan biosorbent[24]	33.27
Activated carbon (AC)[25,26]	18.9–53.7
Mt-spC nanocomposite[27]	156.25
ATP@C nanocomposite[28]	177.74
I@C nanocomposite[2]	149.25
Polypyrrole/Fe_3O_4 magnetic nanocomposite[29]	169.4
Polypyrrole–polyaniline nanofibers[30]	227.0
N-CNS*	256.41

* Present work

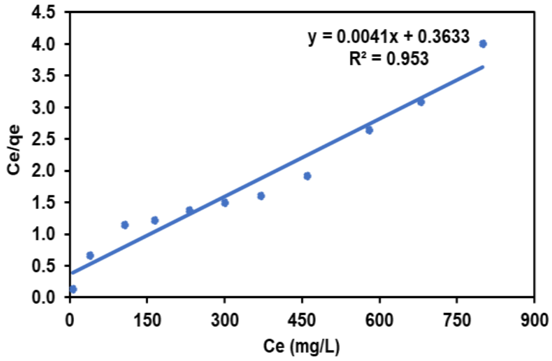

Figure 7: Langmuir adsorption Isotherm.

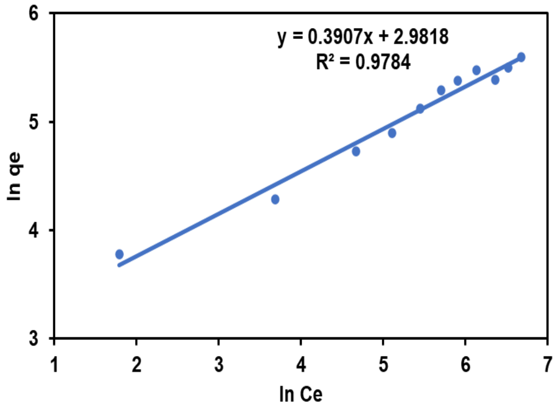

Figure 8: Freundlich adsorption Isotherm.

Conclusion

In the present work, we have covered a variety of N-CNS preparation procedures for aqueous adsorption techniques. N-CNS has both oxygen and nitrogen functional groups in its structure. The most common nitrogen surface functions are pyrrolic-N and pyridinic-N. The adsorptive qualities of N-CNS toward heavy metals and organics depend heavily on these surface functions.

Acknowledgement

All the authors are grateful to the Amity University Uttar Pradesh (AUUP, Noida) for offering a library and research infrastructure. We would also like to express our credit to BIORENDER, for the graphical abstract.

References

1. Ansari M.O. et al, Anion Selective Ptsa Doped Polyaniline@Graphene Oxide-Multiwalled Carbon Nanotube Composite for Cr(VI) and Congo Red Adsorption, *Journal of Colloid And Interface Science*, **496**, 407–415 **(2017)**

2. Ali I. and Gupta V.K., Advances In Water Treatment by Adsorption Technology, *Nature Protocols*, **1**, 2661–2667 **(2007)**

3. Bhaumik M., Maity A., Srinivasu V.V. and Onyango M.S., Enhanced Removal Of Cr(VI) from Aqueous Solution using Polypyrrole/Fe3O4 Magnetic Nanocomposite, *Journal of Hazardous Materials*, **190**, 381–390 **(2011)**

4. Bhaumik M., Maity A., Srinivasu V.V. and Onyango M.S., Removal of Hexavalent Chromium from Aqueous Solution using Polypyrrole-Polyaniline Nanofibers, *Chemical Engineering Journal*, **181–182**, 323–333 **(2012)**

5. Chen L. et al, Flexible Design of Carbon Nanotubes Grown on Carbon Nanofibers By PECVD fo Enhanced Cr(VI) Adsorption Capacity, *Separation and Purification Technology*, **207**, 406–415 **(2018)**

6. Chen W. et al, Investigation On Biomass Nitrogen-Enriched Pyrolysis: Influence of Temperature, *Bioresource Technology*, **249**, 247–253 **(2018)**

7. Chen L.F. et al, Synthesis of An Attapulgite Clay@Carbon Nanocomposite Adsorbent by A Hydrothermal Carbonization Process and Their Application in the Removal of Toxic Metal Ions from Water, *Langmuir*, **27**, 8998–9004 **(2011)**

8. Dhillon Twinkle, Verma Annu and Kumar Vijay, N-acetylcysteine elevates Nrf-2/ARE-regulated antioxidant response and mitochondrial biogenesis in different brain regions of monocrotophos exposed rats, *Res. J. Biotech*., **17(11)**, 63-72 **(2022)**

9. Kasera N., Hall S. and Kolar P., Effect of Surface Modification by Nitrogen-Containing Chemicals on Morphology and Surface Characteristics of N-Doped Pine Bark Biochars, *Journal of Environmental Chemical Engineering*, **9**, 105161 **(2021)**

10. Leng L. et al, Nitrogen Containing Functional Groups of Biochar: An Overview, *Bioresource Technology*, Doi:10.1016/J.Biortech.2019.122286 **(2019)**

11. Li T., Shen J., Huang S., Li N. and Ye M., Hydrothermal Carbonization Synthesis of A Novel Montmorillonite Supported Carbon Nanosphere Adsorbent aor Removal of Cr (VI) From Waste Water, *Applied Clay Science*, **93–94**, 48–55 **(2014)**

12. Liu W.J., Jiang H. and Yu H.Q., Development Of Biochar-Based Functional Materials: toward A Sustainable Platform Carbon Material, *Chemical Reviews*, **115**, 12251–12285 **(2015)**

13. Ma J.C. and Dougherty D.A., The Cation-Π Interaction, *Chemical Reviews*, **97**, 1303–1324, https://Doi.Org/10.1021/Cr9603744 **(1997)**.

14. Niu L., Deng S., Yu G. and Huang J., Efficient Removal of Cu(II), Pb(II), Cr(VI) And As(V) from Aqueous Solution using an Aminated Resin Prepared by Surface-Initiated Atom Transfer Radical Polymerization, *Chemical Engineering Journal*, **165**, 751–757 **(2010)**

15. Rathour R.K.S., Bhattacharya J. and Mukherjee A., Selective and Multicycle Removal of Cr(VI) By Graphene Oxide–EDTA Composite: Insight into the Removal Mechanism and Ionic Interference in Binary and Ternary Associations, *Environmental Technology And Innovation*, **19**, 100851 **(2020)**

16. Setshedi K.Z., Bhaumik M., Onyango M.S. and Maity A., High-Performance Towards Cr(VI) Removal using Multi-Active Sites Of Polypyrrole-Graphene Oxide Nanocomposites: Batch and Column Studies, *Chemical Engineering Journal*, **262**, 921–931 **(2015)**

17. Samuel M.S. et al, Efficient Removal of Chromium(VI) from Aqueous Solution using Chitosan Grafted Graphene Oxide (CS-GO) Nanocomposite, *International Journal of Biological Macromolecules*, **121**, 285–292 **(2019)**

18. Suhag D., Singh A., Chattopadhyay S., Chakrabarti S. and Mukherjee M., Hydrothermal Synthesis of Nitrogen Doped Graphene Nanosheets from Carbon Nanosheets with Enhanced Electrocatalytic Properties, *RSC Advances*, **5**, 39705–39713 **(2015)**

19. Saha B. and Orvig C., Biosorbents for Hexavalent Chromium Elimination from Industrial and Municipal Effluents, *Coordination Chemistry Reviews*, **254**, 2959–2972 **(2010)**

20. Tian Y. et al, Nitrogen Conversion in Relation to NH_3 and HCN During Microwave Pyrolysis of Sewage Sludge, *Environmental Science and Technology*, **47**, 3498–3505 **(2013)**

21. Tuzen M. and Soylak M., Multiwalled Carbon Nanotubes for Speciation Of Chromium In Environmental Samples, *Journal of Hazardous Materials*, **147**, 219–225 **(2007)**

22. Wan Z. et al, Sustainable Impact of Tartaric Acid As Electron Shuttle on Hierarchical Iron-Incorporated Biochar, *Chemical Engineering Journal*, **395**, 125138 **(2020)**

23. Wang G., Wang S., Sun W., Sun Z. and Zheng S., Synthesis of A Novel Illite@Carbon Nanocomposite Adsorbent for Removal of Cr(VI) From Wastewater, *Journal of Environmental Sciences (China)*, **57**, 62–71 **(2017)**

24. Wen Y., Tang Z., Chen Y. and Gu Y., Adsorption of Cr(VI) from Aqueous Solutions using Chitosan-Coated Fly Ash

Composite as Biosorbent, *Chemical Engineering Journal*, **175**, 110–116 **(2011)**

25. Wang W. et al, A Novel Bottom-Up Solvothermal Synthesis of Carbon Nanosheets, *Journal of Materials Chemistry A*, **2**, 2390–2396 **(2014)**

26. Wan Z. et al, Customised Fabrication of Nitrogen-Doped Biochar for Environmental and Energy Applications, *Chemical Engineering Journal*, **401**, 126136 **(2020)**

27. Xu J., Yue J., Niu J. and Chen M., Synergistic Removal of Cr(VI) and Dye Contaminants By 0D/2D Bismuth Molybdate Homojunction Photocatalyst Under Visible Light, *Applied Surface Science*, **484**, 1080–1088 **(2019)**

28. Xu J., Yue J., Niu J. and Chen M., Synergistic Removal of Cr(VI) and Dye Contaminants By 0D/2D Bismuth Molybdate Homojunction Photocatalyst Under Visible Light, *Applied Surface Science*, **484**, 1080–1088 **(2019)**

29. Yuan S., Tan Z. and Huang Q., Migration and Transformation Mechanism of Nitrogen In the Biomass–Biochar–Plant Transport Process, *Renewable and Sustainable Energy Reviews*, **85**, 1–13 **(2018)**

30. Zhang G. et al, Preparation Of Znin2s4 Nanosheet-Coated Cds Nanorod Heterostructures for Efficient Photocatalytic Reduction of Cr(VI), *Applied Catalysis B: Environmental*, **232**, 164–174 **(2018)**

31. Zhang Y.J., Ou J.L., Duan Z.K., Xing Z.J. and Wang Y., Adsorption of Cr(VI) on Bamboo Bark-Based Activated Carbon in the Absence and Presence of Humic Acid, *Colloids and Surfaces A: Physicochemical And Engineering Aspects*, **481**, 108–116 **(2015)**.

(Received 24th March 2023, accepted 30th May 2023)